CrystEngComm

PAPER

View Article Online
View Journal | View Issue

Cite this: *CrystEngComm*, 2018, **20**, 738

Incorporating cuprous-halide clusters and lanthanide clusters to construct Heterometallic cluster organic frameworks with luminescence and gas adsorption properties†

Jin-Hua Liu,[a] Ya-Nan Gu,[a] Yi Chen,[a] Yan-Jie Qi,[a] Xin-Xiong Li *[ab] and Shou-Tian Zheng *[ab]

Received 11th November 2017,
Accepted 27th December 2017

DOI: 10.1039/c7ce01963g

rsc.li/crystengcomm

A series of heterometallic cluster organic frameworks based on cuprous-halide Cu_4I_4 clusters and lanthanide clusters, $[Ln_2(H_2O)_8]_2(Cu_4I_4)(pdc)_4][NO_3]_4$·solvent (**1-Ln**, Ln = Y, Tb, Eu, H_2pdc = 3,5-pyridinedicarboxylic acid), have been successfully synthesized under solvothermal conditions. Single-crystal X-ray diffraction analysis reveals that **1-Ln** show fascinating three-dimensional porous framework structures constructed from two dissimilar types of nanosized coordination cages. Gas sorption measurements indicate that **1-Ln** show moderate gas uptake capacities. The UV/vis spectroscopy measurements reveal that **1-Ln** are a class of potential materials for the removal of $Cr_2O_7^{2-}$ from aqueous solution. Additionally, the luminescence properties of **1-Tb** and **1-Eu** have also been investigated.

Introduction

Cluster organic frameworks, constructed from rigid metal cluster secondary building units (SBUs) and various organic ligands, have been provoking great and continuous interest recently, not only because such materials show intriguing and abundant topological structures but also they have potential applications in optics,[1] magnetism,[2] catalysis[3] and gas storage.[4] Compared with that of single metal ions, the design and assembly of new porous framework materials from rigid metal cluster SBUs is more attractive, mainly due to the following reasons: (1) rigid clusters usually have stable geometries and can maintain their configurations throughout the assembly process, and the structures of the final materials are more predictable and controllable; (2) the use of bigger metal clusters as SBUs can make the pore size larger; (3) the final materials may inherit unique physicochemical properties from the metal cluster SBUs; and (4) metal clusters with different compositions, sizes, and functionalities provide abundant variety of potential SBUs for making cluster organic frameworks. Hitherto, the majority of studies in this area have focused on the syntheses of cluster organic frameworks based on only one type of metal cluster SBU, giving rise to some intriguing framework structures.[5] For example, cluster organic frameworks based on square paddlewheel dimer $[Cu_2(CO_2)_4]$,[5a] triangular $In_3O(CO_2)_3$,[5b] tetrahedral $[Cu_4I_4]$ tetramer,[5c] octahedral tetramer $[Zn_4O(CO_2)]$,[5d] and dodecahedral hexamer $[Zr_6O_4(OH)_4(CO_2)_{12}]$[5e] have been successfully assembled and widely investigated. Additionally, some cluster organic frameworks based on polyoxometalate cluster SBUs have also been created, recently.[6]

Compared with the aforementioned cluster organic frameworks containing only one kind of metal cluster SBU, the exploration of heterometallic cluster organic frameworks consisting of two different metal cluster SBUs is obviously lagged far behind,[7] since different metal clusters usually possess different sizes, shapes, and stabilities, as well as different affinities to various coordination donors, making the preparation of heterometallic cluster organic frameworks more challenging.[8] One feasible and effective synthetic strategy for making heterometallic cluster organic frameworks is to choose a suitable metal cluster to combine with dissimilar clusters *via* an appropriate bifunctional organic ligand.[9] Among common metal clusters, cuprous halide clusters have been receiving increasing attention.[10] We are particularly interested in cubane-like Cu_4I_4 clusters because they are N-affinitive clusters with 4-connected tetrahedral characteristics and can be easily obtained *in situ* in the presence of ligands containing N-donors.[11] Besides, Cu_4I_4 usually exhibits

[a] *State Key Laboratory of Photocatalysis on Energy and Environment, College of Chemistry, Fuzhou University, Fuzhou, Fujian 350108, China.*
E-mail: lxx@fzu.edu.cn, stzheng@fzu.edu.cn
[b] *State Key Laboratory of Structural Chemistry, Fujian Institute of Research on the Structure of Matter and Graduate School of the Chinese Academy of Sciences, Fuzhou, Fujian 350002, China*

† Electronic supplementary information (ESI) available: Synthetic details, structural figures, and spectrum data. CCDC 1559076–1559078. For ESI and crystallographic data in CIF or other electronic format see DOI: 10.1039/c7ce01963g

good stability keeping its tetrahedral configuration during the assembly process with other metal clusters. So far, Cu_4I_4 clusters have been successfully integrated with $[Cu_2(CO_2)_4]$,[9a,b] $In_3O(CO_2)_3$,[9c] $[Zr_6(\mu_3\text{-}OH)_8(OH)_8(COO)_8]$,[9d] $[Cu_6S_6N_6]$,[9e] and $[Zn_8(\mu_4\text{-}O)(COO)_{12}(H_2O)_4]$,[9f] respectively, generating a family of 3d–3d, 3d-main group, and 3d–4d heterometallic cluster organic frameworks with impressive structures.[9] More recently, we introduced a Cu_4I_4 cluster to be incorporated into an Anderson-type POM cluster through a bifunctional ligand and obtained an unprecedented heterometallic cluster organic framework with a multifunctional nature.[12] In addition, some lanthanide clusters have also been employed to combine with Cu_4I_4 for 3d–4f heterometallic cluster organic frameworks.[13] Currently, lanthanide clusters continue to attract intensive research attention for their unique electronic configurations and fascinating luminescence properties.[14] As a continuation of our effort to construct new heterometallic cluster organic frameworks, in this work, we use pyridine-3,5-dicarboxylic acid as a bifunctional ligand and successfully construct three new 3d–4f heterometallic cluster organic frameworks based on Cu_4I_4 cluster and binuclear lanthanide cluster SBUs, namely, $[Ln_2(H_2O)_8]_2(Cu_4I_4)(pdc)_4][NO_3]_4$·solvent (**1-Ln**, Ln = Y, Tb, Eu, H_2pdc = 3,5-pyridinedicarboxylic acid). Notably, **1-Ln** exhibit 3-dimensional framework structures consisting of two types of heterometallic cluster-based coordination cages. Although a number of 3d–4f heterometallic cluster organic frameworks based on cuprous-halide clusters and lanthanide clusters have been reported (Table S1†), heterometallic cluster organic frameworks constructed from different coordination cages are scarce.[13a]

Experimental

Materials and measurements

All reactants and solvents were obtained from commercial sources and used for reactions without further purification. Powder X-ray diffraction (PXRD) analyses were carried out using a Rigaku Ultima IV diffractometer with Cu Kα radiation (λ = 1.54051 Å). Thermogravimetric analysis (TGA) was performed using a Mettler Toledo TGA/SDTA 851e analyzer under an air-flow atmosphere with a heating rate of 10 °C min^{-1} in the temperature range of 30–800 °C. The infrared (IR) spectra were recorded using a Nicolet iS50 at room temperature. Energy-dispersive spectrometry (EDS) analyses were performed using a Hirox SH-4000 M type desktop scanning electron microscope. UV-vis adsorption spectra were collected using a PerkinElmer Lambda 35 spectrophotometer to monitor the exchange process. The ESI-MS spectra measurements were performed in the negative ion mode using an Agilent 6520 Q-TOF LC/MS mass spectrometer coupled to an Agilent 1200 LC system. The ESI-MS sample was prepared by adding 2 mol L^{-1} HF aqueous solution to 5 mL H_2O containing 10 mg crystals dropwise until all solids dissolved. Fluorescence spectra were measured with an Edinburgh Instrument FS980 TCSPC luminescence spectrometer using the polycrystalline samples.

Gas adsorption analysis

Single-component gas measurements were performed with an Accelerated Surface Area and Porosimetry 2020 (ASAP 2020) surface area analyzer. All gases used in the adsorption experiment were of 99.999% purity or higher. The samples of **1-Ln** were completely exchanged by soaking in fresh CH_3OH under ambient conditions for 5 days, and the CH_3OH-exchanged sample was further activated by degassing under high vacuum at 333 K for 5 h to obtain the evacuated sample.

Synthesis of $[Y_2(H_2O)_8]_2(Cu_4I_4)(pdc)_4][NO_3]_4$·solvent (1-Y). $Y(NO_3)_3{\cdot}6H_2O$ (0.10 mmol, 39 mg), CuI (0.26 mmol, 50 mg), H_2pdc (0.24 mmol, 40 mg), and KI (0.24 mmol, 40 mg) were added to an *N*,*N*-dimethylformamide (DMF, 3 mL)/H_2O (3 mL) mixed solvent in a 20 mL vial, and then the mixture was heated at 100 °C for 4 days and cooled to room temperature. Green block crystals of **1-Y** suitable for X-ray diffraction experiments were obtained by filtration, washed with DMF and air-dried. Yield: about 48% (based on H_2pdc). IR (KBr pellet, ν/cm^{-1}): 3076(w), 2920(w), 1638(vs), 1501(w), 1366(vs), 1083(m), 936(m), 820(m), 719(s), 649(m).

Synthesis of $[Tb_2(H_2O)_8]_2(Cu_4I_4)(pdc)_4][NO_3]_4$·solvent (1-Tb). 1-Tb was prepared by a similar procedure to that of **1-Y**, except for the replacement of $Y(NO_3)_3{\cdot}6H_2O$ (0.10 mmol, 39 mg) by $Tb(NO_3)_3{\cdot}6H_2O$ (0.10 mmol, 46 mg). Yield: about 47% (based on H_2pdc). IR (KBr pellet, ν/cm^{-1}): 3065(w), 2927(w), 1627(vs), 1511(w), 1362(vs), 1091(m), 930(m), 826(m), 710(s), 654(m).

Synthesis of $[Eu_2(H_2O)_8]_2(Cu_4I_4)(pdc)_4][NO_3]_4$·solvent (1-Eu). 1-Eu was prepared by a similar procedure to that of **1-Y**, except for the replacement of $Y(NO_3)_3{\cdot}6H_2O$ (0.10 mmol, 39 mg) by $Eu(NO_3)_3{\cdot}6H_2O$ (0.10 mmol, 45 mg). Yield: about 50% (based on H_2pdc). IR (KBr pellet, ν/cm^{-1}): 3077(w), 2933(w), 1627(vs), 1501(w), 1373(vs), 1091(m), 936(m), 831(m), 726(s), 665(m).

Single-crystal structure determination

Single-crystal X-ray diffraction data of **1-Ln** were collected using a Bruker Apex Duo CCD diffractometer with graphite-monochromated Mo Kα radiation (λ = 0.71073 Å) operating at 175 K under a nitrogen atmosphere. The structures of **1-Ln** were solved through direct methods and refined by full-matrix least-squares refinements based on F^2 using the SHELX-2014 program package.[15] All non-hydrogen atoms were refined using anisotropic thermal parameters. The hydrogen atoms of H_2pdc and H_2O were added theoretically to specific atoms. The lanthanide ions in **1-Ln** were disordered and split over two positions. The disordered solvent molecules and charge compensation anions in **1-Ln** were removed using the SQUEEZE[16] program in PLATON. A summary of the crystal data and structure refinements for **1-Ln** is given in

Table 1 Crystal data and structure refinement for **1-Ln**

	1-Y	**1-Tb**	**1-Eu**
Empirical formula	$C_{28}H_{44}Cu_4I_4N_4O_{32}Y_4$	$C_{28}H_{44}Cu_4I_4N_4O_{32}Tb_4$	$C_{28}H_{44}Cu_4I_4N_4O_{32}Eu_4$
Formula weight	2066.07	2346.11	2318.27
Crystal system	Tetragonal	Tetragonal	Tetragonal
Space group	*P*4/*nmm*	*P*4/*nmm*	*P*4/*nmm*
a (Å)	18.52(4)	18.65(14)	18.62(9)
b (Å)	18.52(4)	18.65(14)	18.62(9)
c (Å)	12.30(2)	12.25(19)	12.31(12)
V (Å^3)	4224.2(14)	4264.5(9)	4271.6(6)
Z	2	2	2
F(000)	1960	2168	2152
ρ_{calcd} (g cm^{-3})	1.624	1.827	1.802
Temperature (K)	175(2)	175(2)	175(2)
μ (mm^{-1})	5.223	5.755	5.371
Refl. collected	13 995	14 323	14 062
Independent relf.	2088	2118	2118
Parameters	107	103	103
GOF on F^2	1.005	1.063	1.061
Final *R* indices ($I = 2\sigma(I)$)	$R_1 = 0.0537$, w$R_2 = 0.1746$	$R_1 = 0.0694$, w$R_2 = 0.2145$	$R_1 = 0.0697$, w$R_2 = 0.2167$
R indices (all data)	$R_1 = 0.0631$, w$R_2 = 0.1808$	$R_1 = 0.0803$, w$R_2 = 0.2222$	$R_1 = 0.0768$, w$R_2 = 0.2223$

$R_1 = \sum||F_o| - |F_c||/\sum|F_o|$. w$R_2 = [\sum w(F_o^2 - F_c^2)^2/\sum w(F_o^2)^2]^{1/2}$; $w = 1/[\sigma^2(F_o^2) + (xP)^2 + yP]$, $P = (F_o^2 + 2F_c^2)/3$, where $x = 0.130000$, $y = 12.010800$ for **1-Y**; where $x = 0.124200$, $y = 82.498199$ for **1-Tb**; where $x = 0.131500$, $y = 67.968399$ for **1-Eu**.

Table 1. CCDC 1559076–1559078 contain the supplementary crystallographic data for this paper.

Results and discussion

Crystal structure description

Single-crystal X-ray diffraction analyses reveal that **1-Ln** have isostructural structures containing different lanthanide ions, as evidenced by energy dispersed X-ray spectroscopy (Fig. S1†). Therefore, **1-Y** was used for structural description. **1-Y** crystallizes in a tetragonal system with the *P*4/*nmm* space group, and its asymmetric unit comprises one independent Y^{3+} ion, one Cu^+ ion, one I^-, half of one pdc^{2-} ligand and three coordinated water molecules (Fig. S2†). One of the interesting structural features of **1-Y** is the presence of two dissimilar types of cluster SBUs. The first is cubane-like Cu_4I_4, a conventional cuprous-halide cluster constructed from four tetrahedral coordinated Cu^+ ions bridged by four μ_3-I^- ions. The Cu_4I_4 cluster usually shows a tetrahedral connection characteristic, and it is further stabilized by four N atoms from the pyridyl rings of the pdc^{2-} ligands (Fig. 1a). The Cu–I bond lengths are located in the range of 2.621(18) and 2.734(12) Å and the I–Cu–I bond angles are in the range of 108.78(4) and 120.99(7)°, which are comparable with those of the reported cuprous-halide clusters.[17] The second cluster SBU is the dinuclear lanthanide cluster $[Y_2(pdc)_4(H_2O)_4]^{2-}$ (Fig. 1b). The structure of $[Y_2(pdc)_4(H_2O)_8]^{2-}$ can be viewed as two symmetry-related Y^{3+} ions integrated by four carboxylic groups from four pdc^{2-} ligands, and each Y^{3+} ion is finally terminally ligated by four water molecules. The Y^{3+} ion in $[Y_2(pdc)_4(H_2O)_4]^{2-}$ adopts an eight-connected square antiprismatic geometry, and the Y···Y distance is about 3.452(5) Å. From a structural point of view, such a dinuclear lanthanide cluster is similar to the famous paddlewheel clusters based on divalent transition-metal ions such as Cu^{2+}, Zn^{2+}, Ni^{2+}, Co^{2+}, and so on.[18] So far, divalent transition-metal based paddlewheel clusters have been widely used as SBUs in making various fascinating architectures; however, trivalent lanthanide ion based paddlewheel clusters are relatively uncommon.[19] For the pdc^{2-} ligand, it exhibits a three-connected bridging mode. The pyridyl N atom of the pdc^{2-} ligand connects to one N-affinitive cubane-like Cu_4I_4 cluster, while the two carboxyl groups link two O-affinitive dinuclear lanthanide clusters (Fig. 1c). Such a bridging mode is consistent with the hard and soft (Lewis) acid–base theory.[20]

Another intriguing structural characteristic of **1-Y** is the existence of two types of heterometallic coordination cages with different sizes. The small cage with a size of 1.4 × 1.4 × 1.3 nm^3 consists of four $[Y_2(COO)_4(H_2O)_8]^{2-}$ units, two Cu_4I_4 clusters and four pdc^{2-} ligands (Fig. 1d). Meanwhile, the large cage is constructed from eight $[Y_2(COO)_4(H_2O)_8]^{2-}$ units, four Cu_4I_4 clusters and twelve pdc^{2-} ligands, and its size is about 2.3 × 2.3 × 1.9 nm^3 (Fig. 1e). The inner diameter and calculated pore size based on van der Waals surfaces are about 7.0 Å and 1436.0 Å^3 for the small cage, and the values of those for the large cage are 15.5 Å and 15990.6 Å^3, respectively. These two types of complicated heterometallic coordination cages can also be viewed as a diamondoid cage for the small one and a distorted decahedral cage for the large one when the cluster-based vertexes and the bridging ligands were simplified as different nodes (Fig. 1f and g). So far, coordination cages based on two types of transition-metal clusters have been often observed in reports on cluster organic frameworks. For example, a variety of different heterometallic coordination cages based on $[Zn_4O(COO)_4]^{2+}$ and $[Cu_3(OH)(PyC)_3]^{2+}$ clusters can be found in a porous cluster organic framework reported by Qiaowei Li et. Al.[7a] Similarly, coordination cages built from Cu_4I_4 and $[Cu_2(COO)_4(H_2O)_2]$

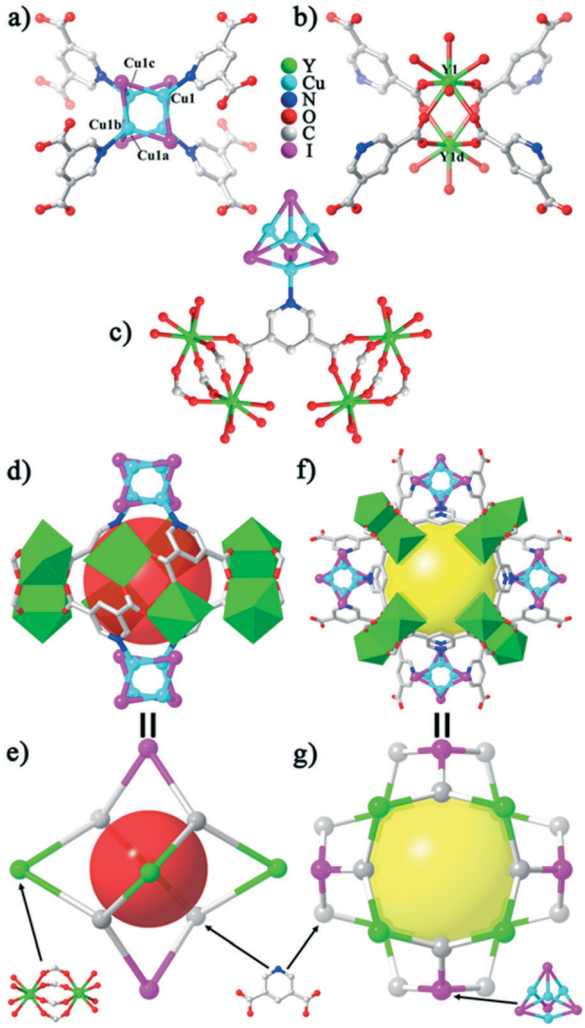

Fig. 1 (a) Illustration of the coordination environment of the Cu_4I_4 cluster. (b) View of the binuclear $[Y_2(pdc)_4(H_2O)_8]^{2-}$ fragment. (c) The coordination mode of the deprotonated pdc^{2-} ligand. (d) View of the small coordination cage based on four $[Y_2(COO)_4(H_2O)_8]^{2-}$ units, two Cu_4I_4 clusters and four pdc^{2-} ligands. (e) View of the large coordination cage built from eight $[Y_2(COO)_4(H_2O)_8]^{2-}$ units, four Cu_4I_4 clusters and twelve pdc^{2-} ligands. (f) Simplified representation of the small coordination cage. (g) Simplified representation of the large coordination cage. All hydrogen atoms were omitted for clarity. Polyhedron color code: YO_8, green.

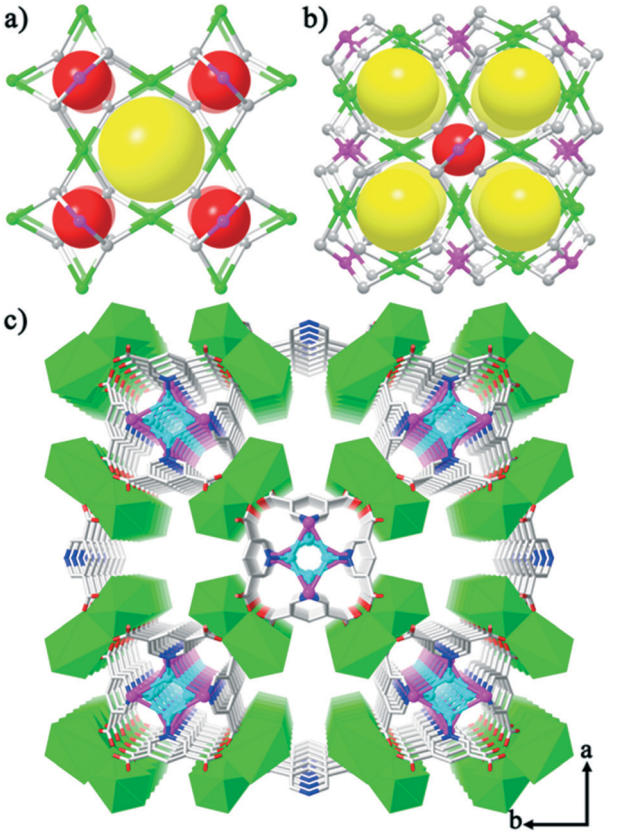

Fig. 2 (a) The connection of the large coordination cage with eight small coordination cages through sharing six-membered windows. (b) The linking mode of the small coordination cage with eight large coordination cages. (c) View the 3D heterometallic framework structure of **1-Ln**.

clusters have been achieved by Guoming Wang et. Al.[9a] Using Cu_4I_4 and $[Zr_6(\mu_3\text{-}OH)_8(OH)_8]^{8+}$ clusters as SBUs, dodecahedral cages with rhombic open faces were designed and constructed by Yuan's group.[9d] Compared with the above cages only based on transition-metal cluster SBUs, to the best of our knowledge, coordination cages consisting of transition-metal cluster SBUs and lanthanide clusters are relatively limited.

The most memorable structural feature that is worth noting is the further assembly of these heterometallic coordination cages. As shown in Fig. S3,† by sharing six-membered windows or vertexes, each distorted decahedral cage joined eight diamondoid cages on the periphery (Fig. 2a), and every diamondoid cage also connected eight decahedral cages (Fig. 2b). The connection of these different cages leads to the construction of a 3D cationic framework which exhibits 1D irregular channels with a size of about 8.6 × 3.5 $Å^2$ along the *c* axis. In the sight of topology, the overall 3D framework can be rationalized as a 3,4,4,-connected 3-nodal network with a Schläfli symbol of $\{6^2\cdot8^2\cdot10^2\}_2\{6^2\cdot8^4\}\{6^3\}_4$ by assigning the pdc^{2-} ligands as 3-connected nodes and the binuclear $[Y_2(COO)_4(H_2O)_8]^{2+}$ moieties and Cu_4I_4 clusters as two kinds of 4-connected nodes (Fig. S4†). The cavities and the channels of the frameworks are filled with disordered NO_3^- charge compensation anions and lattice solvent molecules that cannot be definitely determined in single-crystal X-ray diffraction analysis, which is common in porous structures.[21] The existence of NO_3^- anions in the framework is evidenced by the characteristic vibration band arising from NO_3^- (1374 cm^{-1}),[22] as shown in the IR (Fig. S5†) and electrospray-ionization mass spectrometry spectra (Fig. S6†).

Gas adsorption properties

The agreement of the experimental PXRD patterns with the simulated ones based on single-crystal X-ray diffraction results indicated the good phase purities of **1-Ln** (Fig.

S7†). TGA curves (Fig. S8†) and variable-temperature PXRD patterns also proved that the frameworks of **1-Ln** are still intact up to about 300 °C. PLATON calculation shows that **1-Ln** (Y, Tb, Eu) have 42.2%, 42.0%, and 41.1% potential solvent-accessible void volumes, respectively. The good thermal stability and large potential guest-accessible volumes of **1-Ln** motivated us to further investigate the gas adsorption properties of these porous frameworks. As shown in Fig. 3, the N_2 sorption of **1-Ln** at 77 K exhibits a type **I** isotherm typical of materials with permanent porosity, which verify the retention of microporosity with saturated uptakes of 147.3, 146.28 and 103.4 $cm^3\ g^{-1}$ for **1-Y**, **1-Tb** and **1-Eu**, respectively. These values are not only superior to those for similar Cu_4I_4-based cluster organic frameworks,[23] but also comparable with those for well-known porous materials, InOF-14 (ref. 24) (108 $cm^3\ g^{-1}$) and FJI-7 (ref. 13*b*) (118.5 $cm^3\ g^{-1}$), under the same conditions. The calculated total pore volumes of **1-Y**, **1-Tb** and **1-Eu** based on N_2 sorption are 0.278, 0.216 and 0.117 $cm^3\ g^{-1}$, respectively. The Brunauer–Emmett–Teller (BET) surface area and Langmuir surface area are calculated to be around 545.26 and 639.12 $m^2\ g^{-1}$ for **1-Y**, 524.42 and 593.03 $m^2\ g^{-1}$ for **1-Tb**, and 375 and 427 $m^2\ g^{-1}$ for **1-Eu**, respectively. Additionally, the non-local density functional theory analysis shows that **1-Ln** exhibit a narrow pore distribution of the micropores of about 6.43 Å for **1-Y**, 6.43 Å for **1-Tb** and 7.3 Å for **1-Eu** (Fig. S9†). The CO_2 and H_2 uptake capacities of **1-Ln** were further investigated. **1-Ln** also show reversible type **I** adsorption isotherms at 273 K/298 K and 77 K under 760 mmHg, respectively. The adsorption amounts of CO_2 reach 50.88 and 41.40 $cm^3\ g^{-1}$ for **1-Y**, 61.61 and 44.79 $cm^3\ g^{-1}$ for **1-Tb**, and 40.13 and 22.38 $cm^3\ g^{-1}$ for **1-Eu** at 273 K and 298 K under 760 mmHg, respectively. It is noteworthy that the CO_2 uptake capacity of **1-Tb** is superior to those of some porous metal–organic frameworks such as ZIF-82 (ref. 25) (52.7 $cm^3\ g^{-1}$ at 273 K under 760 mmHg) and CPM-201 (ref. 26) (40.7 $cm^3\ g^{-1}$ at 273 K under 760 mmHg) under the same conditions. The H_2 uptake values of **1-Ln** at 77 K under 760 mmHg are 113.83 $cm^3\ g^{-1}$, 110.23 $cm^3\ g^{-1}$ and 65.58 $cm^3\ g^{-1}$.

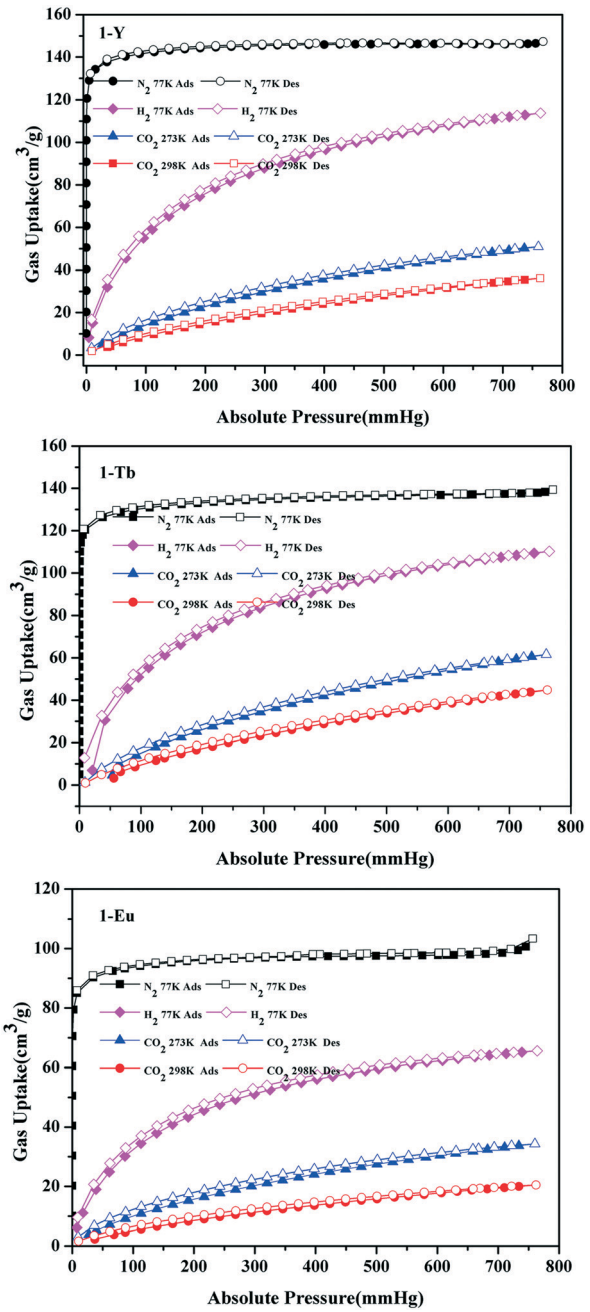

Fig. 3 Gas sorption isotherms of **1-Ln**.

Luminescence properties

On account of the interesting luminescence properties of lanthanide ions and cuprous-halide clusters,[27] the solid-state luminescence properties of **1-Ln** were investigated at room temperature. As depicted in Fig. 4, **1-Tb** shows typical emission peaks at 490, 545, 587 and 622 nm upon excitation at 377 nm (Fig. S10†), which correspond to the 4f–4f electronic transitions from $^5D_4$ excited state to the low-lying ^7F_J levels in the Tb^{3+} cation (J = 6, 5, 4 and 3), respectively. The strongest emission band at 545 nm and two weakest emission bands at 587 and 622 nm are ascribed to $^5D_4 \rightarrow {}^7F_5$ and $^5D_4 \rightarrow {}^7F_4$, $^5D_4 \rightarrow {}^7F_3$, respectively. The emission with moderate intensity at 490 nm is assigned to the $^5D_4 \rightarrow {}^7F_3$ electronic transition.[28] Furthermore, no obvious emission arising from cuprous-halide clusters is observed, which may be attributed to the reason that the emission of cuprous-halide clusters is covered by much stronger peaks from Tb^{3+} cations. For **1-Eu**, it emits characteristic peaks at 593, 614, and 698 nm, which are ascribed to the $^5D_0 \rightarrow {}^7F_1$, $^5D_0 \rightarrow {}^7F_2$, and $^5D_0 \rightarrow {}^7F_4$ electronic transitions. Among these peaks, the intensity of the $^5D_0 \rightarrow {}^7F_2$ transition is stronger than that of the $^5D_0 \rightarrow {}^7F_1$ transition, which implies the absence of inversion symmetry of the Eu^{3+} ion.[29] This result is consistent with the single-crystal X-ray analyses. Notably, the emission spectrum of **1-Eu** shows an obvious upward shift in the region of 650–750 nm, compared with reported results for Eu(III)-MOFs,[30] which may be due

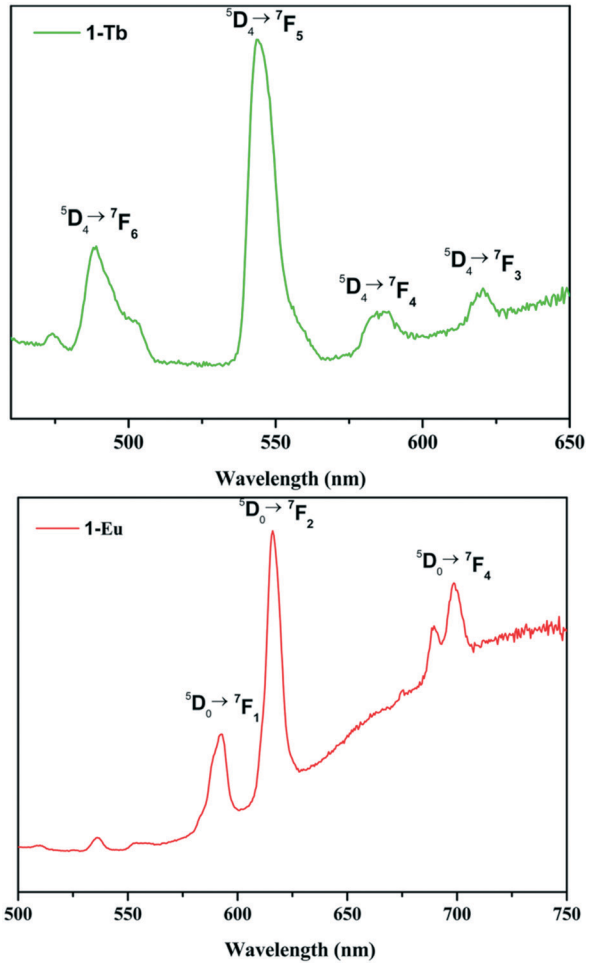

Fig. 4 Solid-state emission spectra of **1-Tb** and **1-Eu** at room temperature.

to the existence of broad emission with weak intensity from copper(I)-halide clusters.

Anion exchange properties

Considering the good stability and the cationic characteristic of the frameworks of **1-Ln**, we chose **1-Y** as an example for anion exchange study. Anion exchange experiments were performed in aqueous solutions using dichromate ($Cr_2O_7^{2-}$) as a model. The exchange process was monitored by UV/vis spectroscopy at intervals based on the intensity variation of the absorption peak of $Cr_2O_7^{2-}$ at 356 nm (ref. 31). As shown in Fig. S11,† when the crystals of **1-Y** were immersed in 10 mL $K_2Cr_2O_7$ aqueous solution with a concentration of 2.0×10^{-4} mol L^{-1}, the $Cr_2O_7^{2-}$ concentration in solution decreased by 72.8% and 87.2% after 6 h and 12 h, respectively, corresponding to capture capacities of 8.2 mg g^{-1} and 9.98 mg g^{-1}, respectively. Subsequently, a slow decrease in the $Cr_2O_7^{2-}$ concentration was observed, and the characteristic peak of $Cr_2O_7^{2-}$ nearly disappeared after 48 h. Simultaneously, the colour of $K_2Cr_2O_7$ aqueous solution changed from yellow to colourless (Fig. S11†). The $Cr_2O_7^{2-}$ concentration in solution decreased by 96.5% after 48 h, and the overall exchange capacity of **1-Y** to exchange $Cr_2O_7^{2-}$ is 10.88 mg g^{-1}. This value is superior to that of the famous inorganic anion exchange material layered double hydroxide (6 mg g^{-1}),[32] and is comparable with that of amino starch (12.12 mg g^{-1}).[33] The PXRD pattern further confirms that the framework of **1-Y** still retains its crystallinity after anion exchange (Fig. S7†).

Conclusions

In summary, using a bifunctional organic ligand H_2pdc as a structural directing agent, a series of heterometallic cluster organic frameworks **1-Ln** based on cuprous-halide cluster SBUs Cu_4I_4 and lanthanide cluster SBUs $[Ln_2(COO)_4(H_2O)_8]^{2+}$ have been successfully prepared under solvothermal conditions. **1-Ln** represent rare examples of heterometallic cluster organic frameworks that contain two types of different nanosized coordination cages. Additionally, **1-Ln** can absorb N_2, H_2 and CO_2 gases with moderate uptake capacities. The present work will not only enrich the structural diversities of heterometallic cluster organic frameworks, but also prove the vast potential for constructing a large number of new functional materials using various cuprous-halide clusters such as Cu_2I_2, Cu_6I_6, and Cu_8I_6, together with lanthanide clusters with different configurations as SBUs.

Conflicts of interest

There are no conflicts to declare.

Acknowledgements

This work was financially supported by the National Natural Science Foundation of China (No. 21371033, 21671040 and 21401195), the Natural Science Foundation For Young Scholars of Fujian Province (No. 2015J05041), and projects from the State Key Laboratory of Structural Chemistry of China (No. 20150001 and 20160020).

Notes and references

1 (*a*) Z. C. Hu, B. J. Deibert and J. Li, *Chem. Soc. Rev.*, 2014, **43**, 5815; (*b*) H. Xu, C. S. Cao, X. M. Kang and B. Zhao, *Dalton Trans.*, 2016, **45**, 18003; (*c*) T. Y. Luo, C. Liu, S. V. Eliseeva, P. F. Muldoon, S. Petoud and N. L. Rosi, *J. Am. Chem. Soc.*, 2017, **139**, 9333; (*d*) Q. F. Zhang, M. Y. Lei, H. Yan, J. Y. Wang and Y. Shi, *Inorg. Chem.*, 2017, **56**, 7610.

2 (*a*) M. Murrie, S. J. Teat, H. Stoeckli-Evans and H. U. Güdel, *Angew. Chem., Int. Ed.*, 2003, **42**, 4653; (*b*) D. W. Ryu, W. R. Lee, J. W. Lee, J. H. Yoon, H. C. Kim, E. K. Kohc and C. S. Hong, *Chem. Commun.*, 2010, **46**, 8779; (*c*) H. C. Hu, X. M. Kang, C. S. Cao, P. Cheng and B. Zhao, *Chem. Commun.*, 2015, **51**, 10850; (*d*) M. Kurmoo, *Chem. Soc. Rev.*, 2009, **38**, 1353; (*e*) Y. L. Hou, G. Xiong, P. F. Shi, R. R. Cheng, J. Z. Cui and B. Zhao, *Chem. Commun.*, 2013, **49**, 6066.

3 (*a*) S. S. Wang and G. Y. Yang, *Chem. Rev.*, 2015, **115**, 4893; (*b*) B. Nohra, H. E. Moll, L. M. R. Albelo, P. Mialane, J.

Marrot, C. Mellot-Draznieks, M. O'Keeffe, R. N. Biboum, J. Lemaire, B. Keita, L. Nadjo and A. Dolbecq, *J. Am. Chem. Soc.*, 2011, **133**, 13363; (*c*) J. C. Wang, Y. H. Hu, G. J. Chen and Y. B. Dong, *Chem. Commun.*, 2016, **52**, 13116.

4 (*a*) J. R. Li, J. M. Yu, W. G. Lu, L. B. Sun, J. Sculley, P. B. Balbuena and H. C. Zhou, *Nat. Commun.*, 2013, **4**, 1538; (*b*) S. T. Zheng, T. Wu, C. Chou, A. Fuhr, P. Y. Feng and X. H. Bu, *J. Am. Chem. Soc.*, 2012, **134**, 4517; (*c*) D. X. Xue, A. J. Cairns, Y. Belmabkhout, L. Wojtas, Y. L. Liu, M. H. Alkordi and M. Eddaoudi, *J. Am. Chem. Soc.*, 2013, **135**, 7660.

5 (*a*) S. S.-Y. Chui, S. M.-F. Lo, J. P. H. Charmant, A. G. Orpen and I. D. Williams, *Science*, 1999, **283**, 1148; (*b*) S. T. Zheng, X. Zhao, S. Lau, A. Fuhr, P. Y. Feng and X. H. Bu, *J. Am. Chem. Soc.*, 2013, **135**, 10270; (*c*) Y. Kang, F. Wang, J. Zhang and X. H. Bu, *J. Am. Chem. Soc.*, 2012, **134**, 17881; (*d*) M. Eddaoudi, J. Kim, N. Rosi, D. Vodak, J. Wachter, M. O'Keeffe and O. M. Yaghi, *Science*, 2002, **295**, 469; (*e*) J. H. Cavka, S. Jakobsen, U. Olsbye, N. Guillou, C. Lamberti, S. Bordiga and K. P. Lillerud, *J. Am. Chem. Soc.*, 2008, **130**, 13850.

6 (*a*) L. M. Rodriguez-Albelo, A. R. Ruiz-Salvador, A. Sampieri, D. W. Lewis, A. Gómez, B. Nohra, P. Mialane, J. Marrot, F. Sécheresse, C. Mellot-Draznieks, R. N. Biboum, B. Keita, L. Nadjo and A. Dolbecq, *J. Am. Chem. Soc.*, 2009, **131**, 16078; (*b*) S. T. Zheng, J. Zhang and G. Y. Yang, *Angew. Chem., Int. Ed.*, 2008, **47**, 3909; (*c*) J. S. Qin, D. Y. Du, W. Guan, X. J. Bo, Y. F. Li, L. P. Guo, Z. M. Su, Y. Y. Wang, Y. Q. Lan and H. C. Zhou, *J. Am. Chem. Soc.*, 2015, **137**, 7169.

7 (*a*) B. B. Tu, Q. Q. Pang, H. S. Xu, X. M. Li, Y. L. Wang, Z. Ma, L. H. Weng and Q. W. Li, *J. Am. Chem. Soc.*, 2017, **139**, 7998; (*b*) B. B. Tu, Q. Q. Pang, E. L. Ning, W. Q. Yan, Y. Qi, D. F. Wu and Q. W. Li, *J. Am. Chem. Soc.*, 2015, **137**, 13456.

8 S. K. Elsaidi, M. H. Mohamed, L. Wojtas, A. J. Cairns, M. Eddaoudiac and M. J. Zaworotko, *Chem. Commun.*, 2013, **49**, 8154.

9 (*a*) G. M. Wang, Z. Z. Xue, J. Pan, L. Wei, S. D. Han, J. J. Qian and Z. H. Wang, *CrystEngComm*, 2016, **18**, 8362; (*b*) S. Yao, X. D. Sun, B. Liu, R. Krishna, G. H. Li, Q. S. Huo and Y. L. Liu, *J. Mater. Chem. A*, 2016, **4**, 15081; (*c*) J. J. Qian, F. L. Jiang, K. Z. Su, J. Pan, Z. Z. Xue, L. F. Liang, P. P. Baga and M. C. Hong, *Chem. Commun.*, 2014, **50**, 15224; (*d*) Y. X. Tan, X. Yang, B. B. Li and D. Q. Yuan, *Chem. Commun.*, 2016, **52**, 13671; (*e*) X. C. Shan, F. L. Jiang, D. Q. Yuan, H. B. Zhang, M. Y. Wu, L. Chen, J. Wei, S. Q. Zhang, J. Pan and M. C. Hong, *Chem. Sci.*, 2013, **4**, 1484; (*f*) Y. X. Tan, Y. P. He and J. Zhang, *Chem. Mater.*, 2012, **24**, 4711.

10 (*a*) P. C. Ford, E. Cariati and J. Bourassa, *Chem. Rev.*, 1999, **99**, 3625; (*b*) Y. Zhang, T. Wu, R. Liu, T. Dou, X. H. Bu and P. Y. Feng, *Cryst. Growth Des.*, 2010, **10**, 2047; (*c*) M. S. Deshmukh, A. Yadav, R. Pant and R. Boomishankar, *Inorg. Chem.*, 2015, **54**, 1337.

11 (*a*) N. X. Zhu, C. W. Zhao, J. C. Wang, Y. A. Li and Y. B. Dong, *Chem. Commun.*, 2016, **52**, 12702; (*b*) Z. X. Fu, J. Lin, L. Li, C. Wang, W. B. Yan and T. Wu, *Cryst. Growth Des.*, 2016, **16**, 2322.

12 X. X. Li, Y. X. Wang, R. H. Wang, C. Y. Cui, C. B. Tian and G. Y. Yang, *Angew. Chem., Int. Ed.*, 2016, **55**, 6462.

13 (*a*) M. B. Zhang, J. Zhang, S. T. Zheng and G. Y. Yang, *Angew. Chem., Int. Ed.*, 2005, **44**, 1385; (*b*) Q. P. Li, P. P. Yu, J. G. Luo and J. G. Qian, *Microporous Mesoporous Mater.*, 2016, **234**, 196; (*c*) X. J. Gu and D. F. Xue, *Cryst. Growth Des.*, 2007, **7**, 1726.

14 (*a*) J. R. Lombardi and B. Davis, *Chem. Rev.*, 2002, **102**, 2431; (*b*) M. Romanelli, G. A. Kumar, T. J. Emge, R. E. Riman and J. G. Brennan, *Angew. Chem., Int. Ed.*, 2008, **47**, 6049; (*c*) R. Sessoli and A. K. Powell, *Coord. Chem. Rev.*, 2009, **253**, 2328; (*d*) M. U. Anwar, S. S. Tandon, L. N. Dawe, F. Habib, M. Murugesu and L. K. Thompson, *Inorg. Chem.*, 2012, **51**, 1028.

15 G. M. Sheldrick, *Acta Crystallogr., Sect. A: Found. Crystallogr.*, 2008, **64**, 112.

16 (*a*) A. L. J. Spek, *Acta Crystallogr., Sect. A: Found. Crystallogr.*, 2003, **36**, 7; (*b*) P. V. D. Sluis and A. L. Spek, *Acta Crystallogr., Sect. A: Found. Crystallogr.*, 1990, **46**, 194.

17 (*a*) S. B. Ren, L. Zhou, J. Zhang, Y. Z. Li, H. B. Du and X. Z. You, *CrystEngComm*, 2009, **11**, 1834; (*b*) S. Naik, J. T. Mague and M. S. Balakrishna, *Inorg. Chem.*, 2014, **53**, 3864; (*c*) K. Fejfarová, K. Kirakci, J. Martinčík, M. Nikl and K. Lang, *Inorg. Chem.*, 2017, **56**, 4609.

18 (*a*) J. T. Li, X. L. Luo, N. Zhao, L. R. Zhang, Q. S. Huo and Y. L. Liu, *Inorg. Chem.*, 2017, **56**, 4141; (*b*) D. N. Dybtsev, H. Chun and K. Kim, *Angew. Chem., Int. Ed.*, 2004, **43**, 5033; (*c*) G. Barin, V. Krungleviciute, D. A. Gomez-Gualdron, A. A. Sarjeant, R. Q. Snurr, J. T. Hupp, T. Yildirim and O. K. Farha, *Chem. Mater.*, 2014, **26**, 1912; (*d*) X. L. Luo, L. B. Sun, J. Zhao, D. S. Li, D. M. Wang, G. G. Li, Q. S. Huo and Y. L. Liu, *Cryst. Growth Des.*, 2015, **15**, 4901.

19 (*a*) D. Y. Ma, H. L. Liu and Y. W. Li, *Inorg. Chem. Commun.*, 2009, **12**, 883; (*b*) Y. Kang, F. Wang and J. Zhang, *Inorg. Chem. Commun.*, 2010, **13**, 938; (*c*) X. Y. Wang, P. F. Yan, Y. X. Li, G. G. An, X. Yao and G. M. Li, *Cryst. Growth Des.*, 2017, **17**, 2178.

20 (*a*) S. Nayak, K. Harms and S. Dehnen, *Inorg. Chem.*, 2011, **50**, 2714; (*b*) Y. Han, H. Zheng, K. Liu, H. L. Wang, H. L. Huang, L. H. Xie, L. Wang and J. R. Li, *ACS Appl. Mater. Interfaces*, 2016, **8**, 23331; (*c*) Y. Sakata, S. Hiraoka and M. Shionoya, *Chem. – Eur. J.*, 2010, **16**, 3318; (*d*) X. J. Gu and D. F. Xue, *Inorg. Chem.*, 2007, **46**, 5349.

21 X. X. Li, H. Y. Xu, F. Z. Kong and R. H. Wang, *Angew. Chem., Int. Ed.*, 2013, **52**, 13769.

22 L. Carlucci, G. Ciani, S. Maggini, D. M. Proserpio and M. Visconti, *Chem. – Eur. J.*, 2010, **16**, 12328.

23 M. M. Siddiqui, S. M. Mobin, I. Senkovska, S. Kaskelc and M. S. Balakrishna, *Chem. Commun.*, 2014, **50**, 12273.

24 J. J. Qian, Q. P. Li, L. F. Liang, Y. Yang, Z. Cao, P. P. Yu, S. M. Huang and M. C. Hong, *Chem. Commun.*, 2016, **52**, 9032.

25 R. Banerjee, H. Furukawa, D. Britt, C. Knobler, M. O'Keeffe and O. M. Yaghi, *J. Am. Chem. Soc.*, 2009, **131**, 3875.

26 Q. G. Zhai, X. H. Bu, X. Zhao, C. Y. Mao, F. Bu, X. T. Chen and P. Y. Feng, *Cryst. Growth Des.*, 2016, **16**, 1261.

27 G. Zeng, S. H. Xing, X. R. Wang, Y. L. Yang, D. X. Ma, H. W. Liang, L. Gao, J. Hua, G. H. Li, Z. Shi and S. H. Feng, *Inorg. Chem.*, 2016, **55**, 1089.

28 (*a*) T. M. Reineke, M. Eddaoudi, M. Fehr, D. Kelley and O. M. Yaghi, *J. Am. Chem. Soc.*, 1999, **121**, 1651; (*b*) B. L. Chen, L. B. Wang, F. Zapata, G. D. Qian and E. B. Lobkovsky, *J. Am. Chem. Soc.*, 2008, **130**, 6718; (*c*) Y. Yang, F. L. Jiang, L. Chen, J. D. Pang, M. Y. Wu, X. Y. Wan, J. Pan, J. J. Qian and M. C. Hong, *J. Mater. Chem. A*, 2015, **3**, 13526.

29 (*a*) Y. Q. Sun, J. Zhang and G. Y. Yang, *Chem. Commun.*, 2006, 4700; (*b*) J. W. Cheng, S. T. Zheng and G. Y. Yang, *Dalton Trans.*, 2007, 4059.

30 (*a*) B. L. Chen, L. B. Wang, Y. Q. Xiao, F. R. Fronczek, M. Xue, Y. J. Cui and G. D. Qian, *Angew. Chem., Int. Ed.*, 2009, **48**, 500; (*b*) Z. H. Li, L. P. Xue, S. B. Miao and B. T. Zhao, *Inorg. Chem. Commun.*, 2011, **14**, 1690.

31 (*a*) C. P. Li, H. Zhou, S. Wang, J. Chen, Z. L. Wang and M. Du, *Chem. Commun.*, 2017, **53**, 9206; (*b*) P. F. Shi, B. Zhao, G. Xiong, Y. L. Hou and P. Cheng, *Chem. Commun.*, 2012, **48**, 8231; (*c*) G. Wojcik, V. Neagu and I. Bunia, *J. Hazard. Mater.*, 2011, **190**, 544.

32 H. Fei, M. R. Bresler and S. R. J. Oliver, *J. Am. Chem. Soc.*, 2011, **133**, 11110.

33 A. Donga, J. Xie, W. Wang, L. Yu, Q. Liu and Y. Yin, *J. Hazard. Mater.*, 2010, **181**, 448.